How accurately should we calibrate a Massive MIMO TDD system?

Xiwen JIANG[*][†], Florian Kaltenberger[*] Luc Deneire[†]

[*]EURECOM, Campus SophiaTech, 06410 Biot, France

[†]Université de Nice Sophia Antipolis, Laboratoire I3S - UMR7271, 06903 Sophia Antipolis, France

`xiwen.jiang@eurecom.fr`

Abstract—We perform an analysis on the accuracy of the channel state information at the transmitter (CSIT) in a Massive MIMO time division duplex (TDD) system. In such a system, channel calibration is needed to compensate the hardware non-symmetry which breaks the TDD channel reciprocity. We consider the joint impact of calibration coefficients and uplink (UL) CSI on the calibrated downlink (DL) CSI accuracy. Moreover, we show the impact of these factors on both conjugate and zero-forcing (ZF) beamforming performance, which provides a useful tool to determine the accuracy level that TDD calibration coefficients should achieve. In this paper, we aim to answer the question: "How accurately should we calibrate a Massive MIMO TDD system to fully release its potential?"

Index Terms—Massive MIMO, TDD, channel reciprocity, calibration, CSIT accuracy.

I. INTRODUCTION

Massive MIMO has been put forward as one of the most promising potential technologies for the 5G mobile network [1] [2]. One of the biggest challenges to fully release its potential is the acquisition of accurate channel state information at the transmitter (CSIT). Conventional procedures to obtain CSIT via feedback from user equipment (UE) will result in heavy overhead in the uplink (UL) in Massive MIMO systems and thus is no longer feasible. Channel reciprocity in time division duplex (TDD) systems became especially attractive to overcome this challenge. Indeed, under a perfect downlink (DL) and UL reciprocity assumption, the base station (BS) can directly apply measured UL channel to its beamforming precoding, and thus UE feedback is avoided. However, this assumption is only true for the physical channel in the air within the coherence time. When the transceiver hardware is taken into consideration, the channel reciprocity is broken since different components are used in transmission and reception radio frequency (RF) chains, hence a calibration mechanism is needed to compensate the hardware non-symmetry.

Calibration solutions to address this problem have existed since a long time ago for traditional TDD systems. In [3], the authors introduced a method to calibrate each RF chain separately with additional hardware component on the transceiver. References [4] and [5] suggested a more cost effective solution via estimating the calibration coefficients by relying on bi-directional measurements between the BS and the UE. This solution can be extended to Massive MIMO, but the cost in the UL to send back accurate channel estimation for all antennas of the BS during the calibration phase is still high, although the calibration process doesn't have to be done very frequently as the calibration parameters stay quite stable during a relatively long time. This concern motivated the authors in [6] to invent a BS internal calibration method for the Argos system by enabling bi-directional transmission between a reference antenna and the rest of the antenna array. BS internal calibration can avoid the involvement of the UE, which results in a common scalar ambiguity for all calibration coefficients, but this ambiguity will not influence the final beamforming performance. [7] extended the Argos method by enabling the transmission between different pairs in the antenna array and getting rid of the reference antenna whose position is very sensitive. This method is especially suitable for distributed Massive MIMO but can also be applied to co-located antenna array. [8] further extended its application in the co-located case by adding weights on different measurements and enabling neighborhood transmission. Noticing that almost all the above calibration algorithms rely on an important assumption that there is no crosstalk between different RF chains and no antenna mutual coupling between different antenna elements, authors in [9] carried out a measurement verification for a small scale multiple-input single-output (MISO) system on EURECOM's OpenAirInterface platform [10], which provides a deep insight into the calibration coefficients in the frequency domain.

Although various calibration methods were provided, little attention has been given to the calibration accuracy needed. From a system design point of view, this topic is essential since it determines how much resources should be used to do the calibration. Consider a practical Massive MIMO TDD system, two different working phases are normally necessary: the calibration phase which is dedicated to estimating calibration coefficients and the beamforming phase when we perform beamforming based on the CSIT inferred from these coefficients and the instantly measured UL CSI. Existing literature studies the impact of the calibration accuracy on the CSIT assuming that the UL channel estimation is perfect, which is not realistic in practice. Simulations of this type can be found in [8] with no closed-form solution provided. [11] gave a beamforming performance analysis of the TDD calibration, but the study was limited to Argos method and zero-forcing (ZF) precoding where the UL channel estimation was again

assumed to be perfect.

In this work, we provide a general closed-form analysis on the DL CSI accuracy, taking into account the impact from both the accuracy of the calibration coefficients and the instantaneous UL channel estimation. We show that when the UL channel estimation is poor, the efforts to improve the calibration coefficients are in vain. Moreover, we will simulate the impact of both factors on the final beamforming performance using conjugate and zero forcing (ZF) precoding. We will show that in high DL signal-to-noise (SNR) region, ZF is more sensitive to the inaccuracy in the estimation of calibration coefficients and UL channel. We provide a method to determine the accuracy level that the calibration coefficients should achieve to guarantee a certain level of beamforming performance.

The rest of this paper is organized as follows: in Sec. II, we introduce the system model and give some basic ideas on how calibration can be done; in Sec. III, we present the CSIT analysis based on calibration coefficients and UL channel estimation; in Sec. IV, we illustrate the impact of both factors on the calibrated CSIT and simulate the beamforming performance. Conclusions are drawn in Sec. V.

Notation: We use upper and lower case boldface letters to denote matrices and vectors respectively. $\mathbb{E}(\cdot)$ is the statistical expectation and $\mathrm{Tr}(\cdot)$ stands for trace. $(\cdot)^*$ is the complex conjugate operation, whereas $(\cdot)^T$ and $(\cdot)^H$ denote the transpose and Hermitian transpose of a vector or a matrix, respectively.

II. SYSTEM MODEL

We use a $M \times 1$ MISO system model as illustrated in Fig. 1, where node A is the BS having M antennas and node B represents a UE with a single antenna. Note that although the MISO model simplifies the analysis, it can also cover multi-user MIMO (MU-MIMO) systems serving single antenna UEs or multi-antenna UEs with negligible antenna mutual coupling, since we can always decompose such a system into several independent MISO systems if we formulate the problem for each independent antenna at the UE side. $\mathbf{T}_A$ (matrix of size $M \times M$) represent the transmission system function at node A from the digital-to-analog converter (DAC) to the antenna array, whereas $\mathbf{R}_A$ denote the node A reception function and includes the characteristics from the antenna array to the analog-to-digital converter (ADC). At node B, the counterparts are represented by t_B and r_B which are scalar since node B has a single antenna. $\mathbf{c}$ denotes the physical channel in the air and is fully reciprocal. $\mathbf{h}_{A \to B}^T$ and $\mathbf{h}_{B \to A}$ are the entire channel seen from the point of view of digital signal processing, which include the hardware and the physical channel in the air and can be represented by

$$\begin{cases} \mathbf{h}_{A \to B}^T = r_B \mathbf{c}^T \mathbf{T}_A \\ \mathbf{h}_{B \to A} = \mathbf{R}_A \mathbf{c} t_B. \end{cases} \tag{1}$$
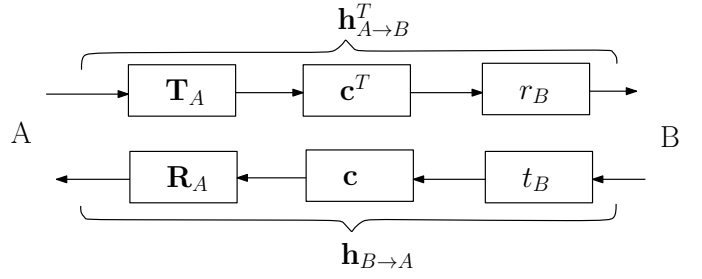
Fig. 1. Reciprocity Model

The relationship between these two channels is given by

$$\begin{aligned} \mathbf{h}_{A \to B}^T &= r_B (\mathbf{R}_A^{-1} \mathbf{h}_{B \to A} t_B^{-1})^T \mathbf{T}_A \\ &= \mathbf{h}_{B \to A}^T \frac{r_B}{t_B} \mathbf{R}_A^{-T} \mathbf{T}_A \\ &= \mathbf{h}_{B \to A}^T \mathbf{F}, \end{aligned} \tag{2}$$

where $\mathbf{F} = \frac{r_B}{t_B} \mathbf{R}_A^{-T} \mathbf{T}_A$ includes all the hardware properties on both sides and is called the calibration matrix.

Different calibration methods are available to estimate $\mathbf{F}$. The method used in [9] consists in collecting N pairs of bi-directional estimation vectors organized in matrices $\hat{\mathbf{H}}_{A \to B} = \left[\hat{\mathbf{h}}_{A \to B}^1, \hat{\mathbf{h}}_{A \to B}^2, \ldots, \hat{\mathbf{h}}_{A \to B}^N\right]^T$ and $\hat{\mathbf{H}}_{B \to A} = \left[\hat{\mathbf{h}}_{B \to A}^1, \hat{\mathbf{h}}_{B \to A}^2, \ldots, \hat{\mathbf{h}}_{B \to A}^N\right]^T$, where $N > M^2$, and formulate a total least square (TLS) estimation problem given by

$$\hat{\mathbf{F}} = \underset{\Delta \mathbf{H}_{B \to A}, \Delta \mathbf{H}_{A \to B}, \mathbf{F}}{\arg \min} \|\Delta \mathbf{H}_{B \to A}\|_{\mathrm{Fro}}^2 + \|\Delta \mathbf{H}_{A \to B}\|_{\mathrm{Fro}}^2$$

$$\text{s.t. } \hat{\mathbf{H}}_{A \to B} - \Delta \mathbf{H}_{A \to B} = (\hat{\mathbf{H}}_{B \to A} - \Delta \mathbf{H}_{B \to A}) \mathbf{F},$$
$$\tag{3}$$

where $\Delta \mathbf{H}_{A \to B}$ and $\Delta \mathbf{H}_{B \to A}$ are the estimation error on channel estimations and $\|\cdot\|_{\mathrm{Fro}}$ is Frobenius norm. The problem can be solved using singular value decompositions (SVD) algorithm. Under the assumption that no RF crosstalk and antenna mutual coupling exist, $\mathbf{F}$ is diagonal and the problem can be decomposed into M independent sub-problems in scalar version. This assumption greatly reduces the calibration complexity and is widely used in other methods, e.g. [6], [7], [8]. The Argos method in [6] gets rid of the involvement of node B and enables a similar bi-directional transmission between a reference antenna and the rest of antenna array inside node A. The methods in [7] and [8] are also internal calibration schemes but the bi-directional transmission is carried out for different antenna pairs.

III. CALIBRATION ACCURACY

In this section we assume that the calibration matrix $\mathbf{F}$ has been estimated during the calibration phase using one of the calibration methods in Sec. II, we are now in the beamforming phase where we apply $\hat{\mathbf{F}}$ to the instantaneous UL channel estimation $\hat{\mathbf{h}}_{B \to A}$ to infer the CSIT $\mathbf{h}_{A \to B}$. The accuracy of the CSIT obtained from such a calibration process depends on three factors: 1) the accuracy of UL channel measurement $\hat{\mathbf{h}}_{B \to A}$, which depends on the channel quality and channel estimator; 2) the accuracy of the estimated relative calibration

$$\overline{\text{MSE}} = \frac{1}{M}\mathbb{E}_{\mathbf{h}_{B\to A},\mathbf{s}_B,\mathbf{N}_A}\left[\|\hat{\mathbf{F}}^T\hat{\mathbf{h}}_{B\to A} - \mathbf{h}_{A\to B}\|^2\right]$$

$$= \frac{1}{M}\mathbb{E}_{\mathbf{h}_{B\to A},\mathbf{s}_B,\mathbf{N}_A}\left[\|\hat{\mathbf{F}}^T\Delta\mathbf{h}_{B\to A} + \Delta\mathbf{F}^T\mathbf{h}_{B\to A}\|^2\right]$$

$$= \frac{1}{M}\text{Tr}\left\{\hat{\mathbf{F}}^T\mathbb{E}_{\mathbf{s}_B,\mathbf{N}_A}\left[\Delta\mathbf{h}_{B\to A}\Delta\mathbf{h}_{B\to A}^H\right]\hat{\mathbf{F}}^* + \Delta\mathbf{F}^T\mathbb{E}_{\mathbf{h}_{B\to A}}\left[\mathbf{h}_{B\to A}\mathbf{h}_{B\to A}^H\right]\Delta\mathbf{F}^*\right\}$$

$$= \frac{1}{M}\text{Tr}\left\{\frac{\sigma_{n,A}^2}{L_B}\hat{\mathbf{F}}^T\hat{\mathbf{F}}^* + \Delta\mathbf{F}^T\mathbf{V}\Delta\mathbf{F}^*\right\} \quad (10)$$

$$= \frac{1}{M}\text{Tr}\left\{\frac{\sigma_{n,A}^2}{L_B}(\mathbf{F}+\Delta\mathbf{F})^T(\mathbf{F}+\Delta\mathbf{F})^* + \Delta\mathbf{F}^T\mathbf{V}\Delta\mathbf{F}^*\right\}$$

$$= \frac{\sigma_{n,A}^2}{ML_B}\text{Tr}\left\{\mathbf{F}^T\mathbf{F}^*\right\} + \frac{1}{M}\text{Tr}\left\{\Delta\mathbf{F}^T\left(\mathbf{V}+\frac{\sigma_{n,A}^2}{L_B}\mathbf{I}\right)\Delta\mathbf{F}^*\right\} + \frac{\sigma_{n,A}^2}{ML_B}\text{Tr}\left\{\mathbf{F}^T\Delta\mathbf{F}^* + \Delta\mathbf{F}^T\mathbf{F}^*\right\}$$

---

matrix $\hat{\mathbf{F}}$, which depends on the calibration method and the number of resources used to do the calibration and 3) the reciprocity level of the UL/DL channel in the air, which is determined by the UL/DL switch time and the channel coherence time. In our analysis, we would not consider the third factor and assume a perfect reciprocity for the UL/DL channel in the air. We perform the theoretical analysis to understand how the first two factors influence the calibrated CSIT accuracy.

A. UL Channel Estimation Error

In the first place, we assume a perfect estimation on the relative calibration matrix, i.e. $\hat{\mathbf{F}} = \mathbf{F}$, and study the influence of the UL channel measurement's quality on the accuracy of CSIT. The signal model for the UL channel estimation at time instant t is given by

$$\mathbf{y}_{A,t} = \mathbf{h}_{B\to A}s_{B,t} + \mathbf{n}_{A,t} \quad (4)$$

where $s_{B,t}$ is the transmitted pilot, $\mathbf{y}_{A,t} \in \mathbb{C}^{M\times1}$ is the received signal at BS, and the noise $\mathbf{n}_{A,t}$ is a vector of circularly-symmetric complex Gaussian random variables following $\mathcal{CN}(0, \sigma_{n,A}^2\mathbf{I})$. Assume that L_B symbols are used for UL channel estimation and stack the transmission for $t = 1, 2, \cdots L_B$, we have

$$\mathbf{Y}_A = \mathbf{h}_{B\to A}\mathbf{s}_B^T + \mathbf{N}_A \quad (5)$$

where $\mathbf{Y}_A \in \mathbb{C}^{M\times T_B}$, $\mathbf{s}_B^T \in \mathbb{C}^{1\times L_B}$, $\mathbf{N}_A \in \mathbb{C}^{M\times L_B}$ are obtained by arranging the corresponding vectors in columns. We adopt the LS estimator as

$$\hat{\mathbf{h}}_{B\to A} = \mathbf{Y}_A\frac{\mathbf{s}_B^*}{\|\mathbf{s}_B\|^2}. \quad (6)$$

Using the estimated channel and the estimation error $\Delta\mathbf{h}_{B\to A}$, Eq. (2) can be rewritten as

$$\mathbf{h}_{A\to B}^T = (\hat{\mathbf{h}}_{B\to A}^T - \Delta\mathbf{h}_{B\to A}^T)\mathbf{F} \quad (7)$$

As LS estimators are linear, $\Delta\mathbf{h}_{B\to A}$ remain circularly-symmetric Gaussian vector. Given that the normalized transmitted symbols on different time slots are i.i.d variables with unit power, i.e. $\mathbb{E}[s_{B,t_1}s_{B,t_2}] = \delta(t_1 - t_2)$ where δ is the Kronecker delta, the variance (with regard to transmitted pilot and noise) of the channel estimators is

$$\mathbb{E}_{\mathbf{s}_B,\mathbf{N}_A}\left[\Delta\mathbf{h}_{B\to A}\Delta\mathbf{h}_{B\to A}^H\right] = \frac{\sigma_{n,A}^2}{L_B}\mathbf{I}. \quad (8)$$

The mean square error (MSE) of the calibrated channel averaged by the number of BS antennas is

$$\overline{\text{MSE}} = \frac{1}{M}\mathbb{E}_{\mathbf{s}_B,\mathbf{N}_A}\left[\|\mathbf{h}_{A\to B} - \mathbf{F}^T\hat{\mathbf{h}}_{B\to A}\|^2\right]$$

$$= \frac{1}{M}\mathbb{E}_{\mathbf{s}_B,\mathbf{N}_A}\left[\text{Tr}\left\{(\mathbf{F}^T\Delta\mathbf{h}_{B\to A})(\mathbf{F}^T\Delta\mathbf{h}_{B\to A})^H\right\}\right] \quad (9)$$

$$= \text{Tr}\left\{\mathbf{F}^T\mathbb{E}_{\mathbf{S}_A,\mathbf{N}_A}\left[\Delta\mathbf{h}_{B\to A}\Delta\mathbf{h}_{B\to A}^H\right]\mathbf{F}^*\right\}$$

$$= \frac{\sigma_{n,A}^2}{ML_B}\text{Tr}\left\{\mathbf{F}^T\mathbf{F}^*\right\}$$

where $\text{Tr}\{\cdot\}$ is the trace of a matrix.

B. Relative Calibration Matrix Estimation Error

Now let us additionally consider the second factor, the accuracy of $\hat{\mathbf{F}}$ and study its impact on the calibrated CSIT's accuracy. The error of $\hat{\mathbf{F}}$ stems from two aspects: 1) approximation error which comes from the simplification on $\mathbf{F}$, e.g. assuming $\mathbf{F}$ is diagonal; 2) estimation error on $\mathbf{F}$, which can be caused by the bi-directional channel estimation inaccuracy during the calibration phase and the variation of $\mathbf{F}$. Indeed, even with perfect instantaneous bi-directional channel estimations, the small variation of the hardware circuits can cause an imperfect calibration matrix estimation in two ways: on the one hand, the real $\mathbf{F}$ during the beamforming phase varies from that in the calibration phase; on the other hand, $\mathbf{F}$ estimation is usually carried out in a certain time interval during which $\mathbf{F}$ is slightly varying as well, thus the obtained $\hat{\mathbf{F}}$ is an average value. Considering $\Delta\mathbf{F}$ as the error of $\mathbf{F}$, i.e. $\hat{\mathbf{F}} = \mathbf{F}+\Delta\mathbf{F}$, and note $\mathbf{V}$ the covariance matrix of the channel from B to A, i.e. $\mathbf{V} = \mathbb{E}\left[\mathbf{h}_{B\to A}\mathbf{h}_{B\to A}^H\right]$, we can represent the averaged MSE of calibrated CSIT by Eq. (10).

The first term in Eq. (10) is the same as in Eq. (9), which is purely due to the UL channel estimation error, and the rest

is the additional error brought in by considering the error on $\hat{\mathbf{F}}$. Note that if we assume $\mathbf{F}$ to be diagonal, then the error $\Delta\mathbf{F} = \Delta\mathbf{F}_d + \mathbf{F}_o$, where $\Delta\mathbf{F}_d$ represents the estimation error on the diagonal elements and $\mathbf{F}_o$ is the approximation error by ignoring the off-diagonal elements.

IV. SIMULATION RESULTS

In this section, we define models for $\mathbf{T}_A$, $\mathbf{R}_A$, t_B, r_B, based on which we calculate the calibration matrix $\mathbf{F}$. We also model the channel in the air $\mathbf{c}$ for a co-located Massive MIMO system using a geometry based Rician channel. We illustrate how the calibration matrix inaccuracy and the error in the UL channel estimation impact the CSIT accuracy. Additionally we also perform simulations to view their final impact on beamforming performance. For these objectives, we use a BS operating at 2.6GHz with a 8×8 square antenna array whose elements are separated by half of the wavelength.

A. Hardware non-symmetry model and channel model

For $\mathbf{T}_A$, $\mathbf{R}_A$, as antenna spacing in our antenna configuration is at least half of the wavelength, the antenna mutual coupling can be neglected [12] [9] and the off-diagonal elements can thus be assumed to be 0. The diagonal elements in $\mathbf{T}_A$, $\mathbf{R}_A$, as well as t_B and r_B, are modeled as i.i.d. random variables, with uniformly distributed phase between $[-\pi \ \pi]$ and independent magnitude uniformly distributed on $[1-\epsilon \ 1+\epsilon]$, with ϵ chosen such that the standard deviation of the squared-magnitudes is 0.1, as in [8] and [13]. Based on this model, we can easily obtain the calibration matrix $\mathbf{F}$ using $\mathbf{F} = \frac{r_B}{t_B}\mathbf{R}_A^{-T}\mathbf{T}_A$.

Moreover, for the channel in the air $\mathbf{c}$, we use a geometry based normalized Rician channel model as in [14] given by

$$\mathbf{c} = \sqrt{K}\mathbf{c}_{\text{LOS}} + \sqrt{1-K}\mathbf{c}_{\text{diffuse}}, \quad (10)$$

where $\mathbf{c}_{\text{LOS}}$ is the line-of-sight component, the elements of which have a unit amplitude and geometry based phase (i.e. the phase is calculated according to radio's incidence angle from UE, thus depends on the relative position of the UE and the antenna element in space); $\mathbf{c}_{\text{diffuse}}$ is the diffuse component corresponding to the standard i.i.d. Rayleigh distribution $\mathcal{CN}(0, \mathbf{I})$; and K is the linear Rician K factor.

B. Simulation Results on the CSIT MSE

Let's first study the impact of calibration matrix accuracy and UL channel estimation on the MSE of CSIT. To obtain a general result, we don't specify the specific calibration method used, thus the elements in $\Delta\mathbf{F}_d$ are assumed to be i.i.d. circularly-symmetric Gaussian variables following $\mathcal{CN}\left(0, \sigma^2_{\Delta\mathbf{F}_d}\right)$. The $\mathbf{F}_d$ estimation quality can be evaluated by the normalized MSE defined as

$$\text{MSE}_{\mathbf{F}_d} = \frac{\|\Delta\mathbf{F}_d\|_D^2}{\|\mathbf{F}_d\|_D^2} = \frac{M\sigma^2_{\Delta\mathbf{F}_d}}{\|\mathbf{F}_d\|_D^2} \quad (11)$$

where $\|(\cdot)\|_D$ represents the norm of the diagonal vector. For UL, we use $L_B = 10$ symbols as the pilots to estimate the UL channel. The K factor in the channel model Eq. (10) is 0,
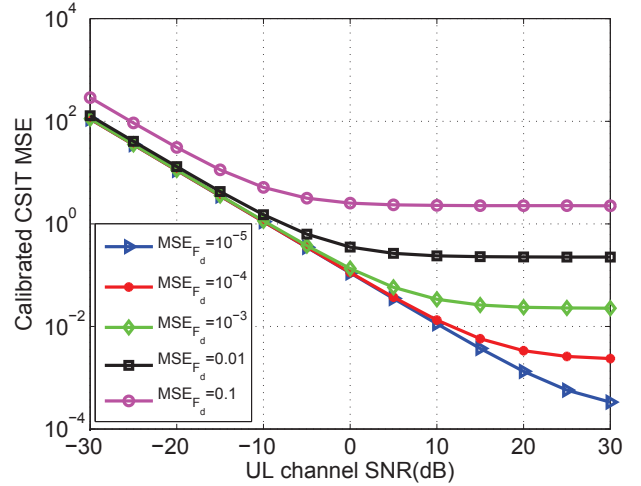
Fig. 2. Calibrated CSIT averaged MSE as a function of UL estimation accuracy and calibration matrix accuracy in a 64×1 MISO system ($L_B = 10$).

i.e. standard Rayleigh channel is used. Under this assumption, the covariance matrix of $\mathbf{h}_{B\to A}$ is $\mathbf{V} = |t_B|^2\mathbf{R}_A\mathbf{R}_A^H$.

The MSE of calibrated CSIT is shown in Fig. 2. We observe that the improvement of calibration matrix accuracy and UL channel estimation can both enhance the accuracy of CSIT. When the UL channel SNR is low, the curves for $\text{MSE}_{\mathbf{F}_d}$ from 0.01 to 10^{-5} almost overlap each other, meaning that the accuracy of UL channel estimation is limiting the calibrated CSIT accuracy and improving $\hat{\mathbf{F}}$ accuracy will be useless. On the other hand, when the UL channel SNR is sufficiently high, the accuracy on the calibration matrix become the limiting factors and all curves become flat. In this case, improving the UL channel estimation accuracy has no further contribution. Furthermore, when the accuracy of $\hat{\mathbf{F}}$ is poor, the corresponding calibration CSIT accuracy curve become flat at a relatively low SNR.

C. Simulation Results on Beamforming Performance

The signal model for the ith user in a MU-MIMO system is given by

$$y_i = \mathbf{h}_i^T\mathbf{w}_i x_i + \sum_{j\neq i}\mathbf{h}_i^T\mathbf{w}_j x_j + \mathbf{n}_i \quad (12)$$

where x_i and y_i are the transmitted and received signal for the ith user. The transmission power is set to 1. $\mathbf{w}_i$ and $\mathbf{h}_i^T = r_{B,i}\mathbf{c}_i^T\mathbf{T}_A$ are the corresponding precoding weights and the channel from the BS to the ith user respectively. We use conjugate and ZF beamforming in this simulation. For conjugate beamforming, $\mathbf{w}_i = \hat{\mathbf{h}}_i^*/\|\hat{\mathbf{h}}_i\|$ with $\hat{\mathbf{h}}_i$ being the estimated DL channel, whereas for ZF, $\mathbf{w}_i = \hat{\mathbf{h}}_i^*(\hat{\mathbf{h}}_i^T\hat{\mathbf{h}}_i^*)^{-1}/\eta$, where η is the normalizing factor keeping the transmission power for each UE being 1. Note that the first term in Eq. (12) is the desired signal, the second term is the interference stemming from the transmission for other users and $\mathbf{n}_i$ is the circularly-symmetric complex Gaussian noise following $\mathcal{CN}(0, \sigma^2_{n,i}\mathbf{I})$.
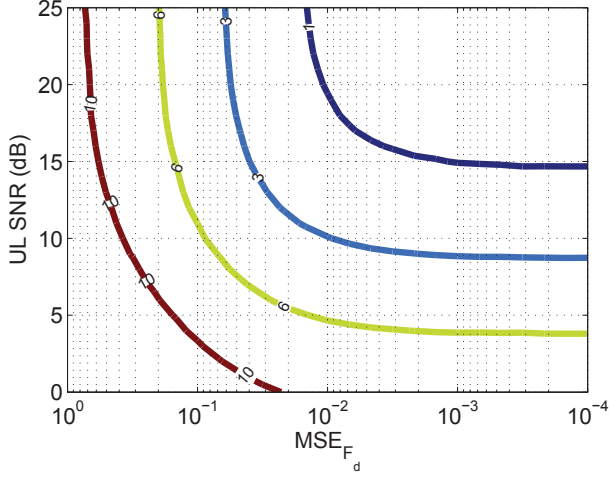
Fig. 3. Conjugate beamforming SINR loss (in dB) due to joint impact of $\hat{\mathbf{F}}$ and UL channel estimation inaccuracy in a 64×8 system with DL SNR=0dB ($L_B = 10$).
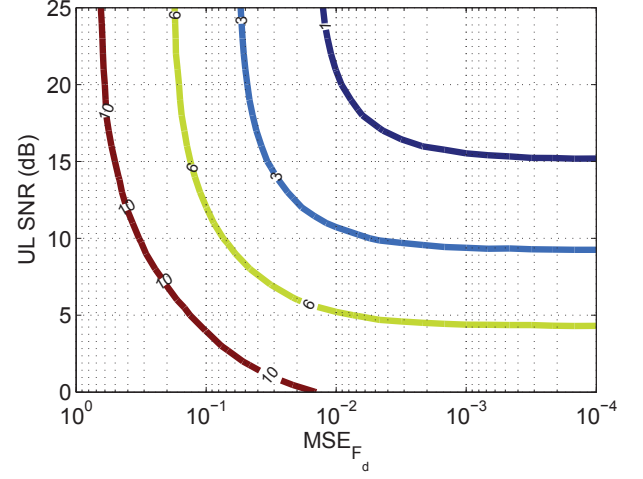
Fig. 5. ZF beamforming SINR loss (in dB) due to joint impact of $\hat{\mathbf{F}}$ and UL channel estimation inaccuracy in a 64×8 system with DL SNR=0dB ($L_B = 10$).
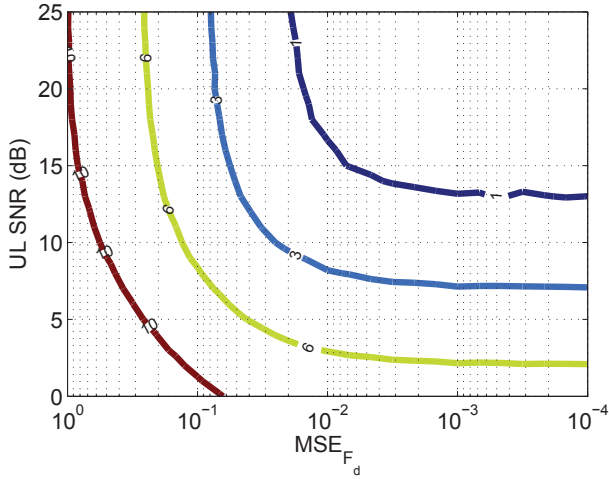
Fig. 4. Conjugate beamforming SINR loss (in dB) due to joint impact of $\hat{\mathbf{F}}$ and UL channel estimation inaccuracy in a 64×8 system with DL SNR=20dB ($L_B = 10$).
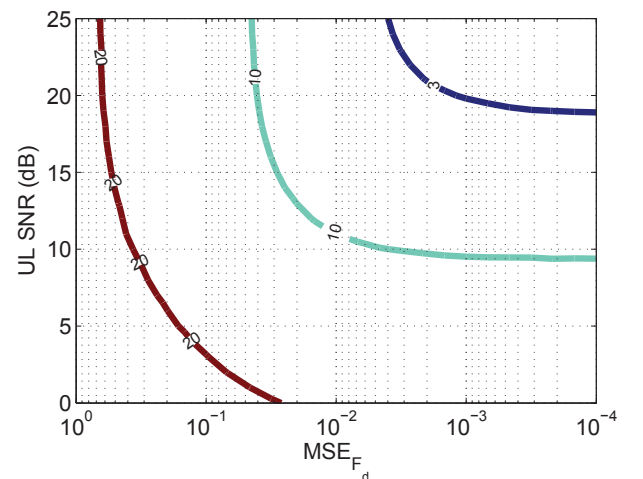
Fig. 6. ZF beamforming SINR loss (in dB) due to joint impact of $\hat{\mathbf{F}}$ and UL channel estimation inaccuracy in a 64×8 system with DL SNR=20dB ($L_B = 10$).

The signal-to-interference-plus-noise ratio (SINR) for user i is given by

$$\text{SINR}_i = \frac{\mathbb{E}\left[\|\mathbf{h}_i^T \mathbf{w}_i\|^2\right]}{\mathbb{E}\left[\|\sum_{j \neq i} \mathbf{h}_i^T \mathbf{w}_j\|^2\right] + \sigma_{n,i}^2}, \tag{13}$$

We use the same antenna array as defined in the beginning of this section and investigate a 64×8 MU-MIMO system. The K-factor in Eq. (10) is set to be 0.5. SINR loss with regard to a perfect CSIT will be used as the performance indicator, which is given by

$$\text{SINR}_{\text{loss},i} = \frac{\text{SINR}_{\text{ideal},i}}{\text{SINR}_i}, \tag{14}$$

where $\text{SINR}_{\text{ideal},i}$ is also calculated using Eq. (13) but with

$\mathbf{w}_i$ and $\mathbf{w}_j$ obtained with perfect channel estimation $\mathbf{h}_i$ and $\mathbf{h}_j$, rather than their estimated values.

Figs. 3–6 illustrate the conjugate and ZF beamforming SINR loss (in dB) due to joint impact of the inaccuracy in $\hat{\mathbf{F}}$ and UL channel estimation for both DL SNR = 20dB ($\sigma_{n,i}^2 = 0.01$) and DL SNR = 0dB ($\sigma_{n,i}^2 = 1$) cases. Different contours in these figures indicate certain values of SINR losses for corresponding $\hat{\mathbf{F}}$ accuracy and UL channel SNR.

We observe that when DL SNR is low (Fig. 3 and 5), the beamforming performance degradation due to TDD reciprocity calibration inaccuracy is similar for conjugate and ZF beamforming, whereas when DL SNR is high (Fig. 4 and 6), ZF beamforming is much more sensitive to the calibration matrix and UL channel estimation inaccuracy. For the latter

case where DL SNR=20dB, let's take an example in which $\text{MSE}_{\mathbf{F}_d} = 10^{-2}$ and UL SNR = 10dB, conjugate beamforming has less than 3dB SINR loss whereas for ZF, this loss is even above 10dB.

Furthermore the joint impact illustration on the SINR loss also offers a useful tool to determine the calibration matrix accuracy we need to achieve if we define an acceptable SINR loss value. Let us still focus on the case where DL SNR = 20dB, assume that UL SNR = 20dB, 10 UL symbols are used to perform UL channel estimation and the acceptable SINR loss due to non-perfect CSIT is defined to be 3dB, for conjugate beamforming, $\text{MSE}_{\mathbf{F}_d}$ less than 0.07 is sufficient whereas for ZF, a $\text{MSE}_{\mathbf{F}_d}$ less than 10^{-3} is needed, which means much more efforts are needed during the calibration process if ZF is used.

V. CONCLUSION

In this paper, we address the problem on how accurately we should calibrate a TDD Massive MIMO system. We perform theoretical analysis on the impact of calibration matrix and UL channel estimation on the CSIT accuracy. We observe that both of them can become a limiting factor, and the CSIT accuracy can be improved only when we allocate more resources on the limiting element. We also perform simulation to study the joint impact of these two factors on both conjugate and ZF beamforming performance. The study shows that ZF is more sensitive to inaccuracy in the calibration matrix and UL channel estimation, especially in high DL SNR region. At the same time, we provide a method to determine the accuracy level that the calibration matrix should achieve to guarantee a certain level of beamforming performance, which can be a useful tool for system design.

ACKNOWLEDGMENTS

REFERENCES

[1] T. Marzetta, "Noncooperative cellular wireless with unlimited numbers of base station antennas," *IEEE Trans. Wireless Commu.*, vol. 9, no. 11, pp. 3590–3600, Nov. 2010.

[2] E. Larsson, O. Edfors, F. Tufvesson, and T. Marzetta, "Massive MIMO for next generation wireless systems," *IEEE Commun. Mag.*, vol. 52, no. 2, pp. 186–195, Feb. 2014.

[3] A. Bourdoux, B. Come, and N. Khaled, "Non-reciprocal transceivers in OFDM/SDMA systems: Impact and mitigation," in *Proc. IEEE Radio and Wireless Conference, (RAWCON)*, Boston, MA, USA, Aug. 2003, pp. 183–186.

[4] M. Guillaud, D. Slock, and R. Knopp, "A practical method for wireless channel reciprocity exploitation through relative calibration," in *Proc. International Symp. Signal Processing and Its Applications (ISSPA)*, Sydney, Australia, Aug. 2005, pp. 403–406.

[5] F. Kaltenberger, H. Jiang, M. Guillaud, and R. Knopp, "Relative channel reciprocity calibration in MIMO/TDD systems," in *Future Network and Mobile Summit*, Florence, Italy, Jun. 2010, pp. 1–10.

[6] C. Shepard, N. Yu, H.and Anand, E. Li, T. Marzetta, R. Yang, and L. Zhong, "Argos: Practical many-antenna base stations," in *Proc. ACM International Conf. Mobile computing and networking (Mobicom)*, Istanbul, Turkey, Aug. 2012, pp. 53–64.

[7] R. Rogalin, O. Bursalioglu, H. Papadopoulos, G. Caire, A. Molisch, A. Michaloliakos, V. Balan, and K. Psounis, "Scalable synchronization and reciprocity calibration for distributed multiuser MIMO," *IEEE Trans. Wireless Commu.*, vol. 13, no. 4, pp. 1815–1831, Apr. 2014.

[8] J. Vieira, F. Rusek, and F. Tufvesson, "Reciprocity calibration methods for Massive MIMO based on antenna coupling," in *Proc. IEEE Global Communications Conference (GLOBECOM)*, Austin, USA, 2014, pp. 3708–3712.

[9] X. Jiang, M. Čirkić, F. Kaltenberger, G. L. Larsson, L. Deneire, and R. Knoppe, "MIMO-TDD reciprocity and hardware imbalances: Experimental results," in *Proc. IEEE International Conference on Communications (ICC)*, London, United Kingdom, Jun. 2015, pp. 4949–4953.

[10] N. Nikaein, R. Knopp, F. Kaltenberger, L. Gauthier, C. Bonnet, D. Nussbaum, and R. Ghaddab, "Demo: Openairinterface: An open LTE network in a PC," in *Proc. ACM International Conf. Mobile Computing and Networking (MobiCom)*, Maui, Hawaii, USA, 2014, pp. 305–308.

[11] D. Liu, W. Ma, S. Shao, Y. Shen, and Y. Tang, "Performance analysis of TDD reciprocity calibration for Massive MU-MIMO systems with ZF beamforming," *Communications Letters, IEEE*, to appear.

[12] M. Petermann, M. Stefer, F. Ludwig, D. Wübben, M. Schneider, S. Paul, and K. Kammeyer, "Multi-user pre-processing in multi-antenna OFDM TDD systems with non-reciprocal transceivers," *IEEE Trans. Commu.*, vol. 61, no. 9, pp. 3781–3793, Sep. 2013.

[13] R. Rogalin, O. Y. Bursalioglu, H. C. Papadopoulos, G. Caire, and A. F. Molisch, "Hardware-impairment compensation for enabling distributed large-scale MIMO," in *Information Theory and Applications Workshop (ITA), 2013*, San Diego, California, USA., Feb. 2013, pp. 1–10.

[14] S. Blandino, F. Kaltenberger, and M. Feilen, "Wireless channel simulator testbed for airborne receivers," in *WI-UAV 2015, 6th International Workshop on Wireless Networking, Control and Positioning for Unmanned Autonomous Vehicles, co-located with IEEE International Conference on Global Communications (GLOBECOM 2015)*, San Diego, USA, Dec. 2015, to appear. [Online]. Available: http://www.eurecom.fr/publication/4702